Supplemental Information for:

Aqueous oxidation of isoprene-derived organosulfates as a source of atmospheric formic and acetic acids

Kelvin H. Bates[1,2,†], Daniel J. Jacob,[2] James D. Cope[1], Xin Chen[3,‡], Dylan B. Millet[3], and Tran B. Nguyen[1]*

1. Department of Environmental Toxicology, University of California Davis, Davis, CA 95616, United States
2. School of Engineering and Applied Sciences, Harvard University, Cambridge, MA, USA
3. Department of Soil, Water, and Climate, University of Minnesota, St. Paul, Minnesota 55108, United States

† Now at: NOAA Chemical Sciences Laboratory, Earth System Research Laboratories, and Cooperative Institute for Research in Environmental Sciences, University of Colorado, Boulder, CO 80305, United States

‡ Now at: Department of Civil and Environmental Engineering, Massachusetts Institute of Technology, Cambridge, MA 02139, United States

*Correspondence to: tbn@ucdavis.edu

Contents:

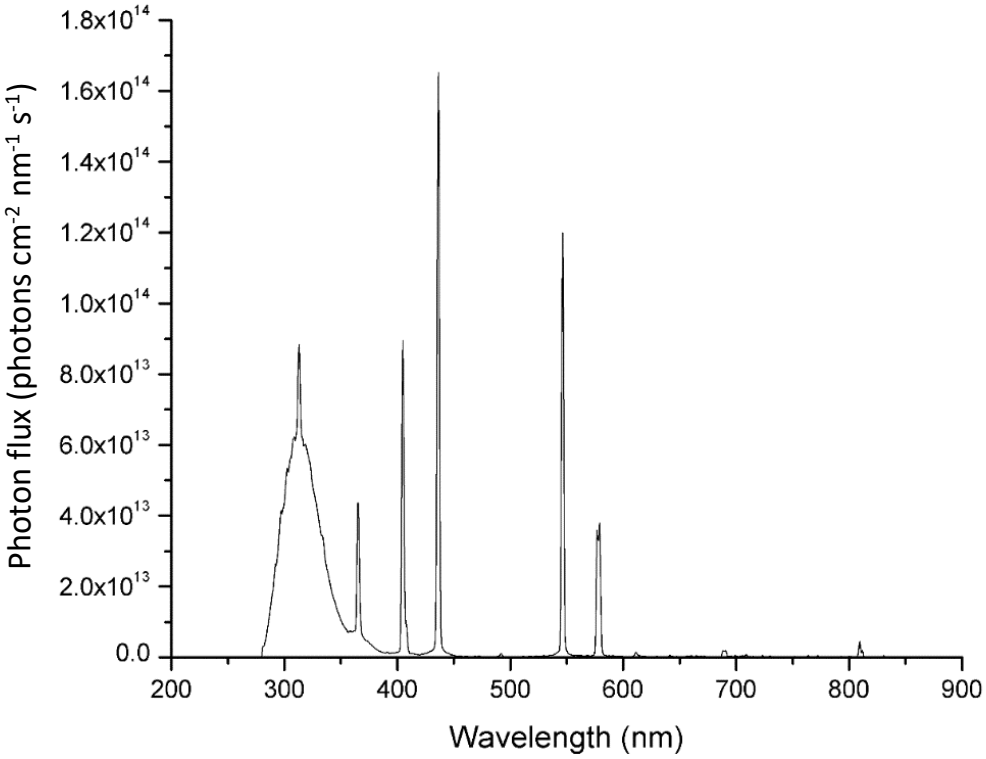

Figure S1. Measured photon flux in the photochemical reaction enclosure, as used in kinetic modeling.

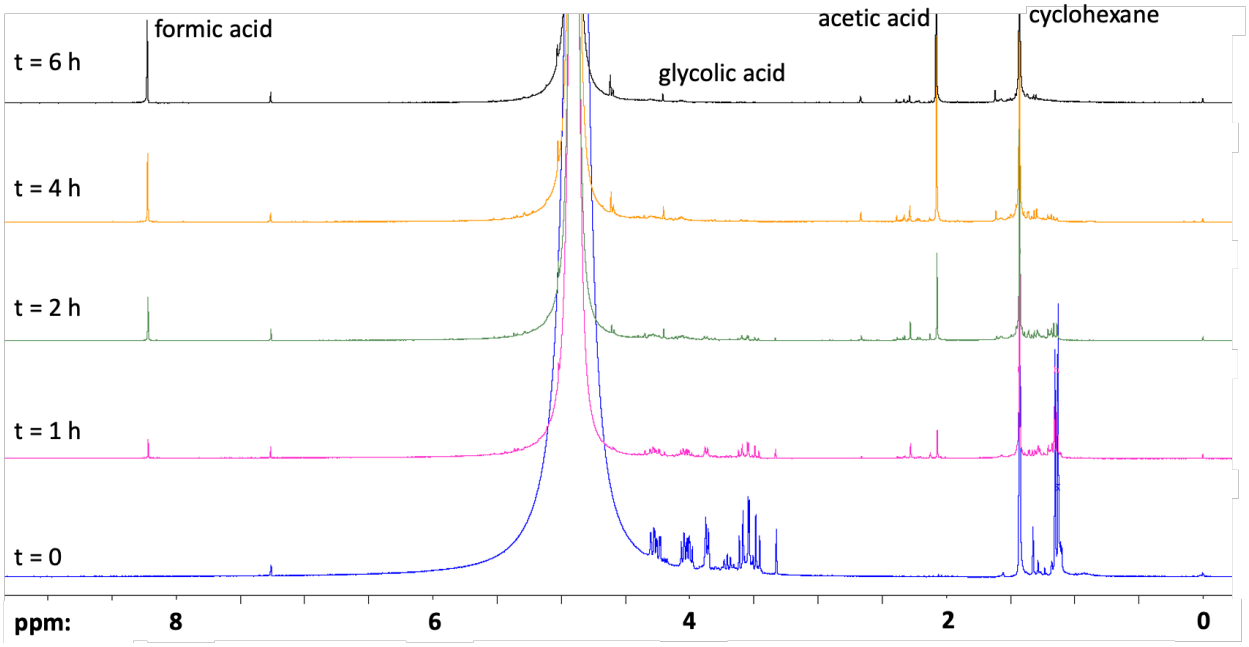

Figure S2. Example NMR spectra during the aqueous photooxidation of 2-MTS. Unlabeled peaks at chemical shifts of 1-1.5 ppm and 3-4.5 ppm represent the starting material, while unlabeled peaks at 2.25-2.75 ppm and 4.5-4.75 ppm represent minor unidentified products.

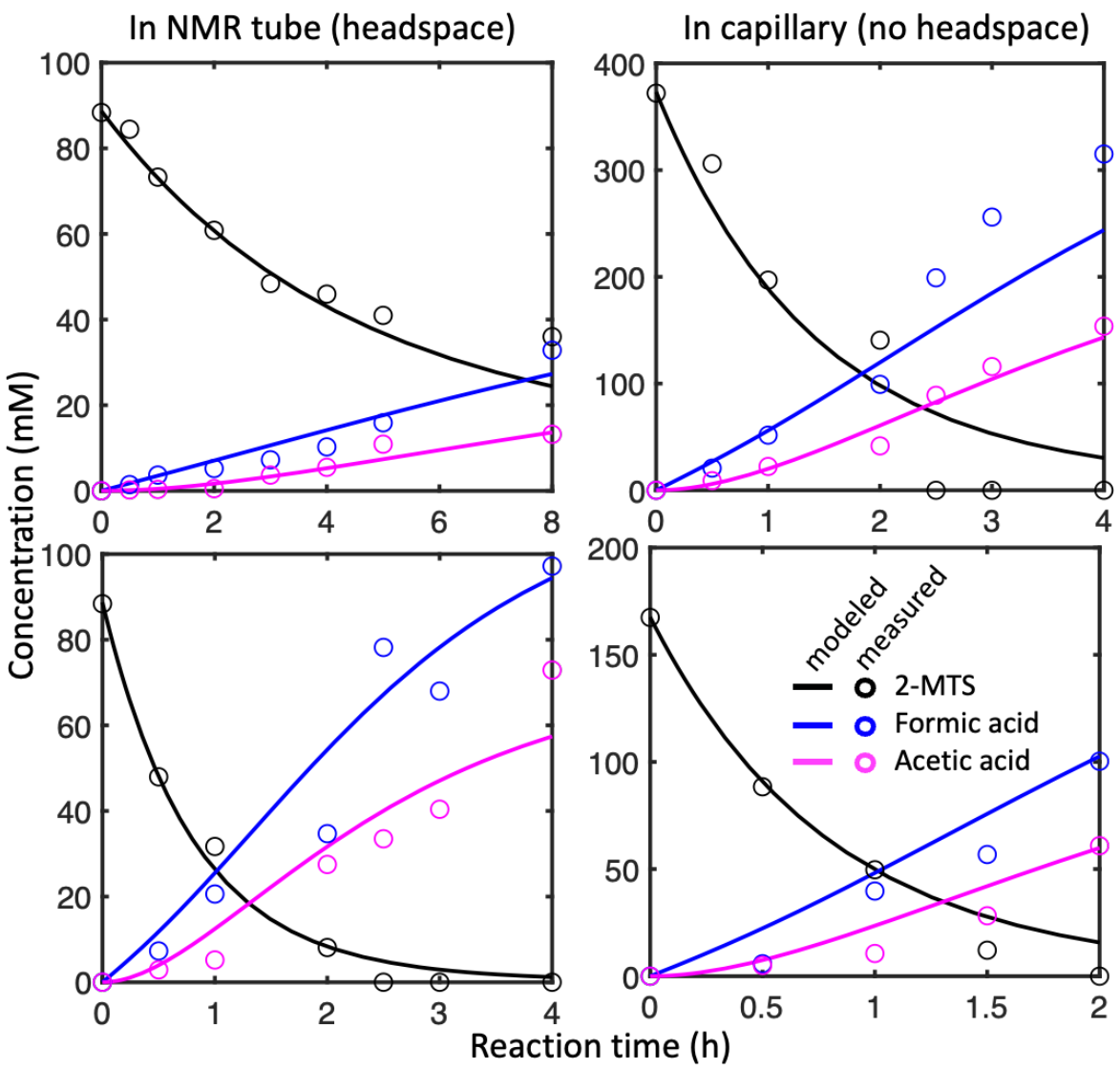

Figure S3. Measured (by ^{1}H NMR) and modeled (using Mechanism S1 in the kinetic model) 2-MTS, formic acid, and acetic acid concentrations in the four individual kinetic experiments. Experiments on the left were performed with the reaction mixture (2-MTS and H_2O_2 in D_2O) in the NMR tube and the standard (cyclohexane in $CDCl_3$) in a sealed glass capillary within the tube, leaving a headspace of air above the reaction mixture. Experiments on the right were performed with the reaction mixture sealed in the glass capillary (without headspace) within the solution of cyclohexane in $CDCl_3$ in the NMR tube. Differences between replicate experiments (top vs. bottom) are from changes in initial 2-MTS concentrations and in light flux.

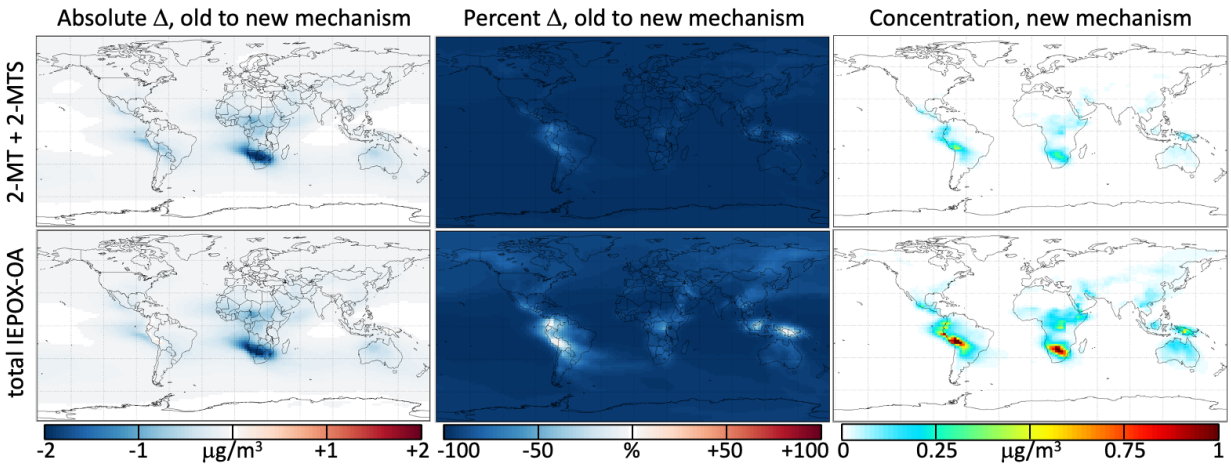

Figure S4. Like Figure 4 in the main text, but for 3 – 10 km altitude instead of 0 – 1 km altitude: IEPOX-derived organic aerosol (IEPOX-OA) and changes in IEPOX-OA concentrations between the base GEOS-Chem mechanism and the updated mechanism with 2-MT and 2-MTS oxidation. Panels show the absolute change between the mechanisms (left), the percent changes between the mechanisms (center), and the absolute concentrations in the updated mechanism (right) for both 2-MT + 2-MTS concentrations (top) and total IEPOX-OA concentrations (bottom). All maps show annual averages at 3 – 10 km altitude.

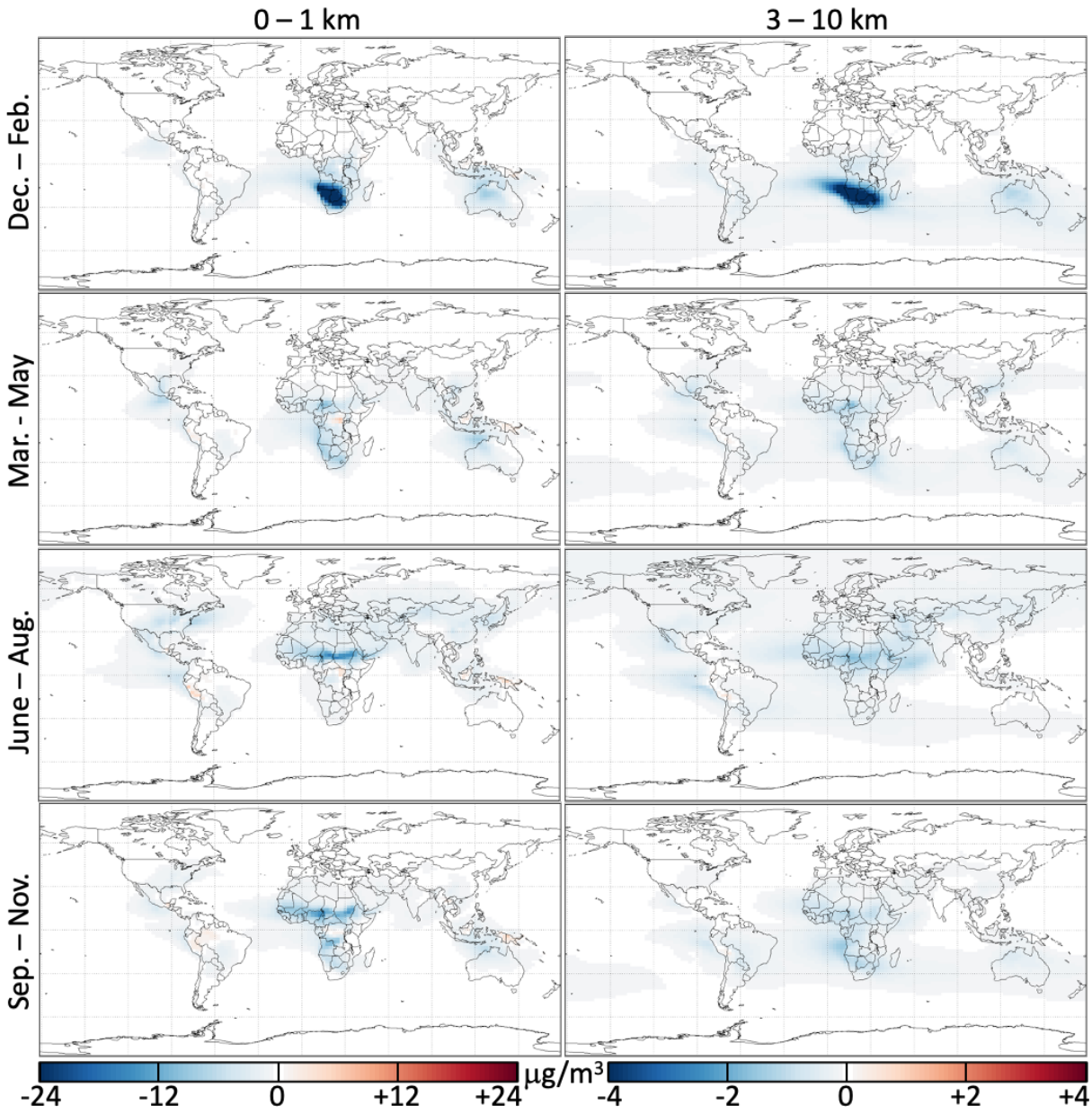

Figure S5. Absolute changes in the seasonal average concentrations of total IEPOX-derived organic aerosol (including 2-MT, 2-MTS, and their particle-phase oxidation products) between simulations with the base GEOS-Chem mechanism and the updated mechanism including 2-MT and 2-MTS oxidation.

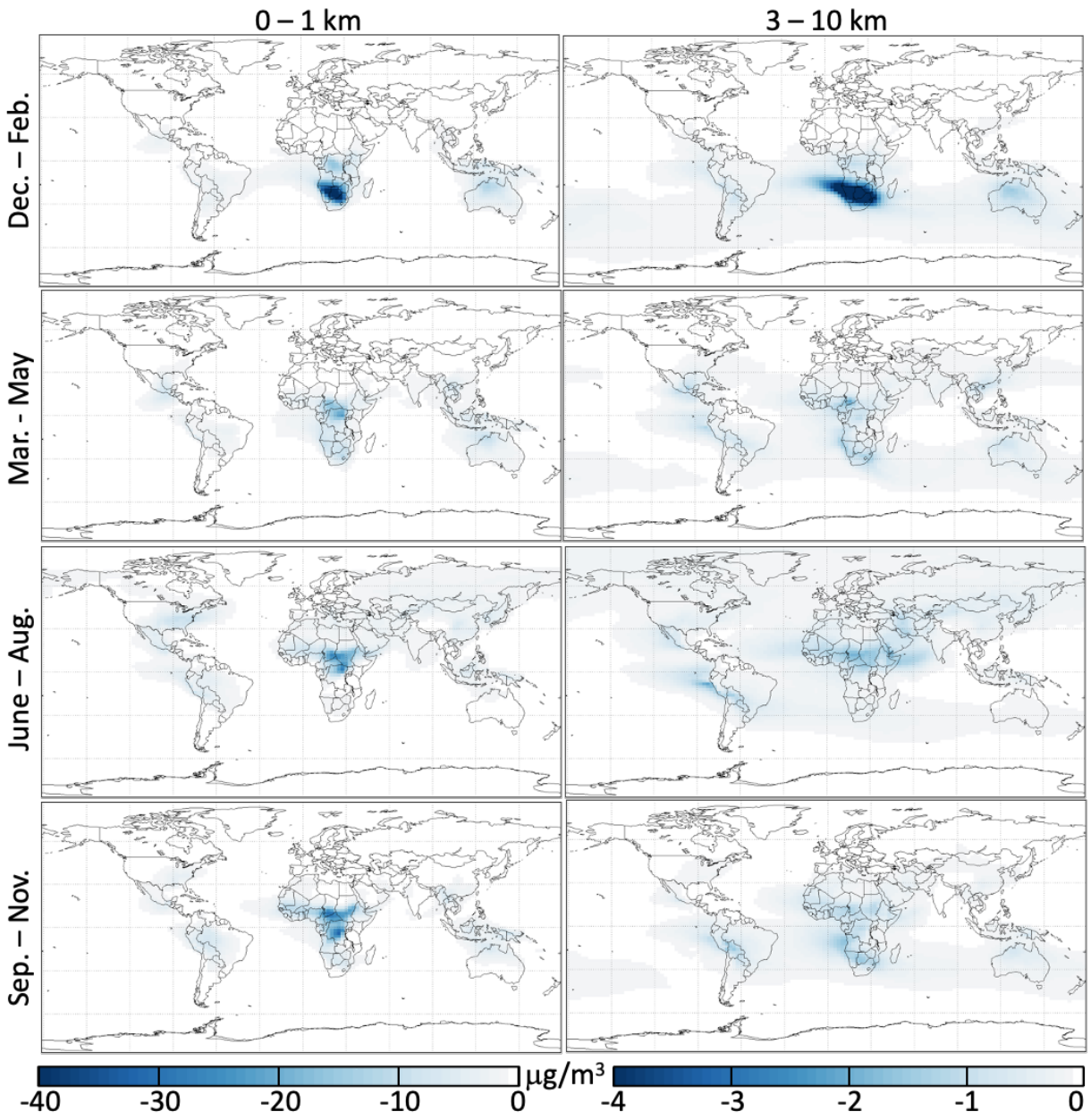

Figure S6. Absolute changes in the seasonal average concentrations of first-generation IEPOX-derived organic aerosol (including only 2-MT and 2-MTS) between simulations with the base GEOS-Chem mechanism and the updated mechanism including 2-MT and 2-MTS oxidation.

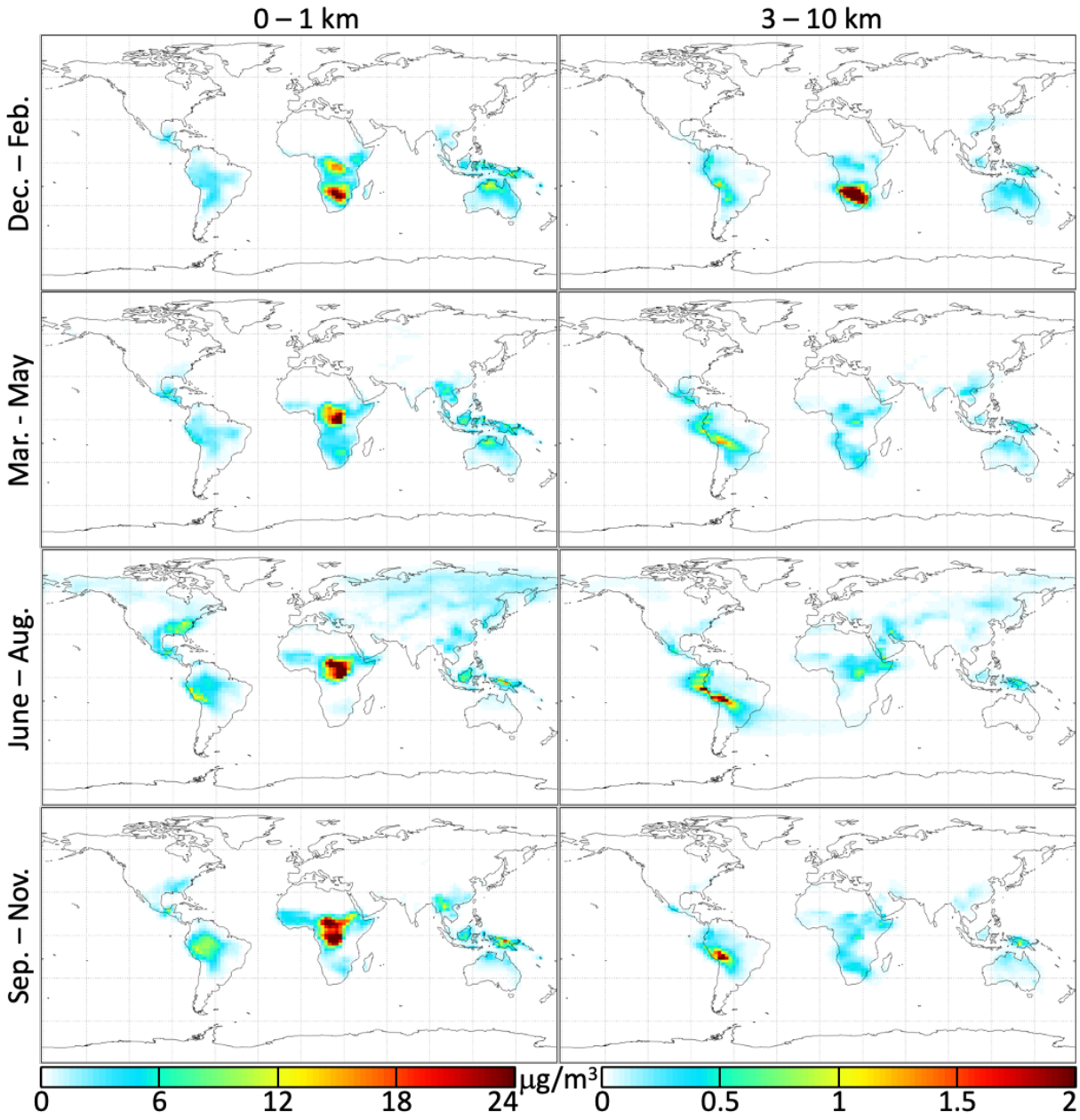

Figure S7. Seasonal average concentrations of total IEPOX-derived organic aerosol (including 2-MT, 2-MTS, and their particle-phase oxidation products) in simulations with the updated mechanism GEOS-Chem mechanism that includes 2-MT and 2-MTS oxidation.

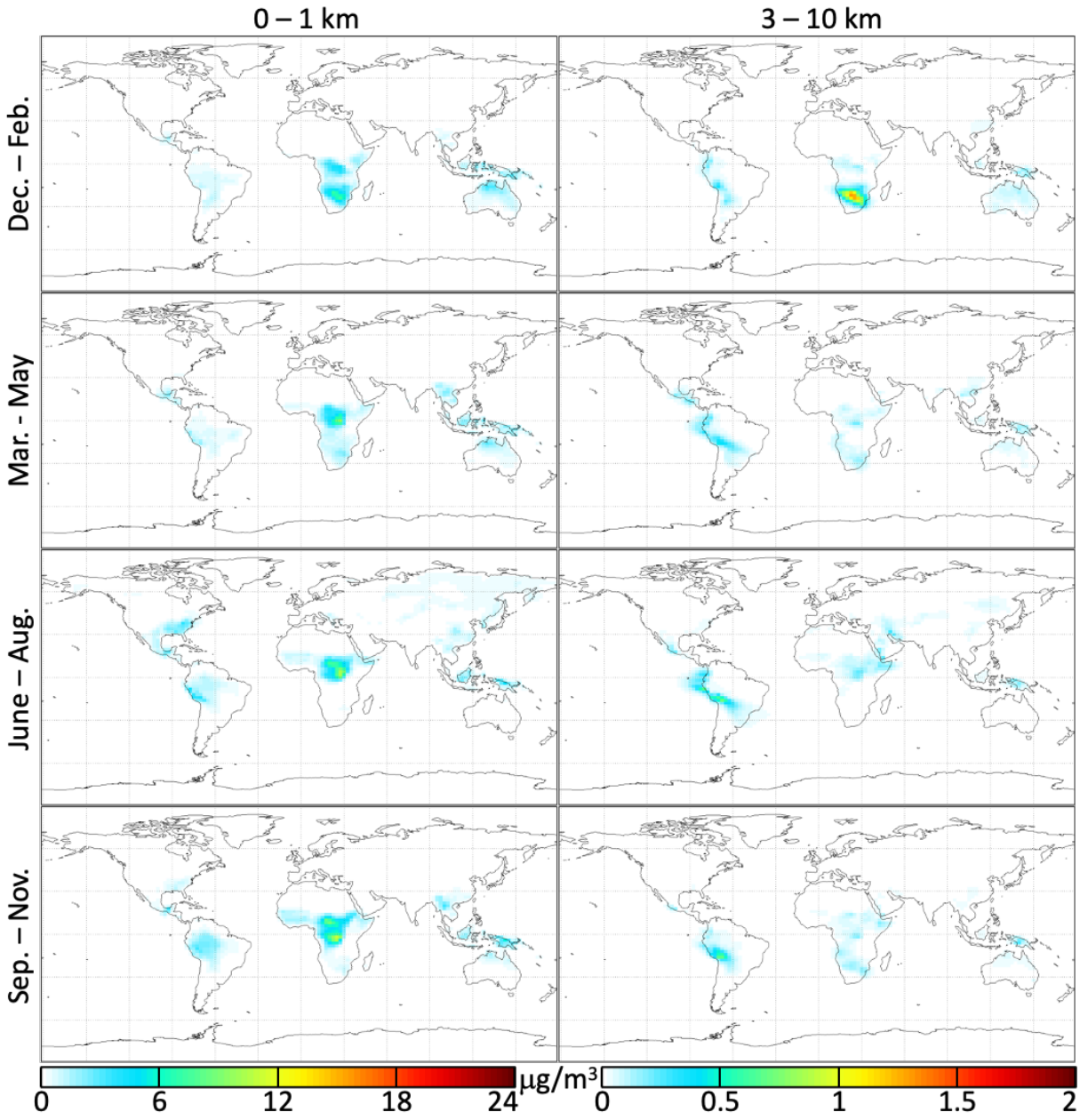

Figure S8. Seasonal average concentrations of first-generation IEPOX-derived organic aerosol (including only 2-MT and 2-MTS) in simulations with the updated mechanism GEOS-Chem mechanism that includes 2-MT and 2-MTS oxidation. Color scales are the same as in Figure S7.

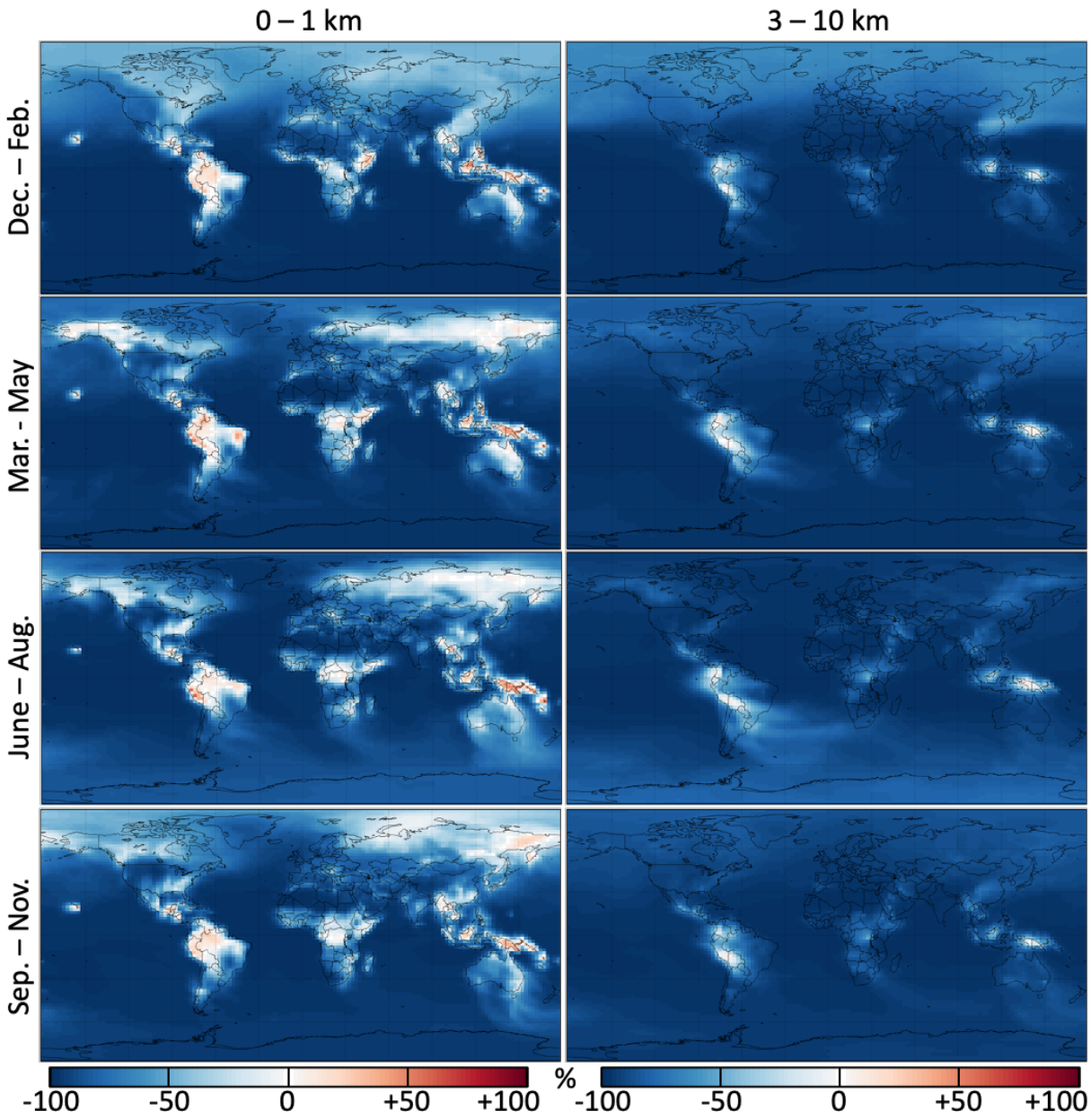

Figure S9. Percent changes in the seasonal average concentrations of total IEPOX-derived organic aerosol (including 2-MT, 2-MTS, and their particle-phase oxidation products) between simulations with the base GEOS-Chem mechanism and the updated mechanism including 2-MT and 2-MTS oxidation.

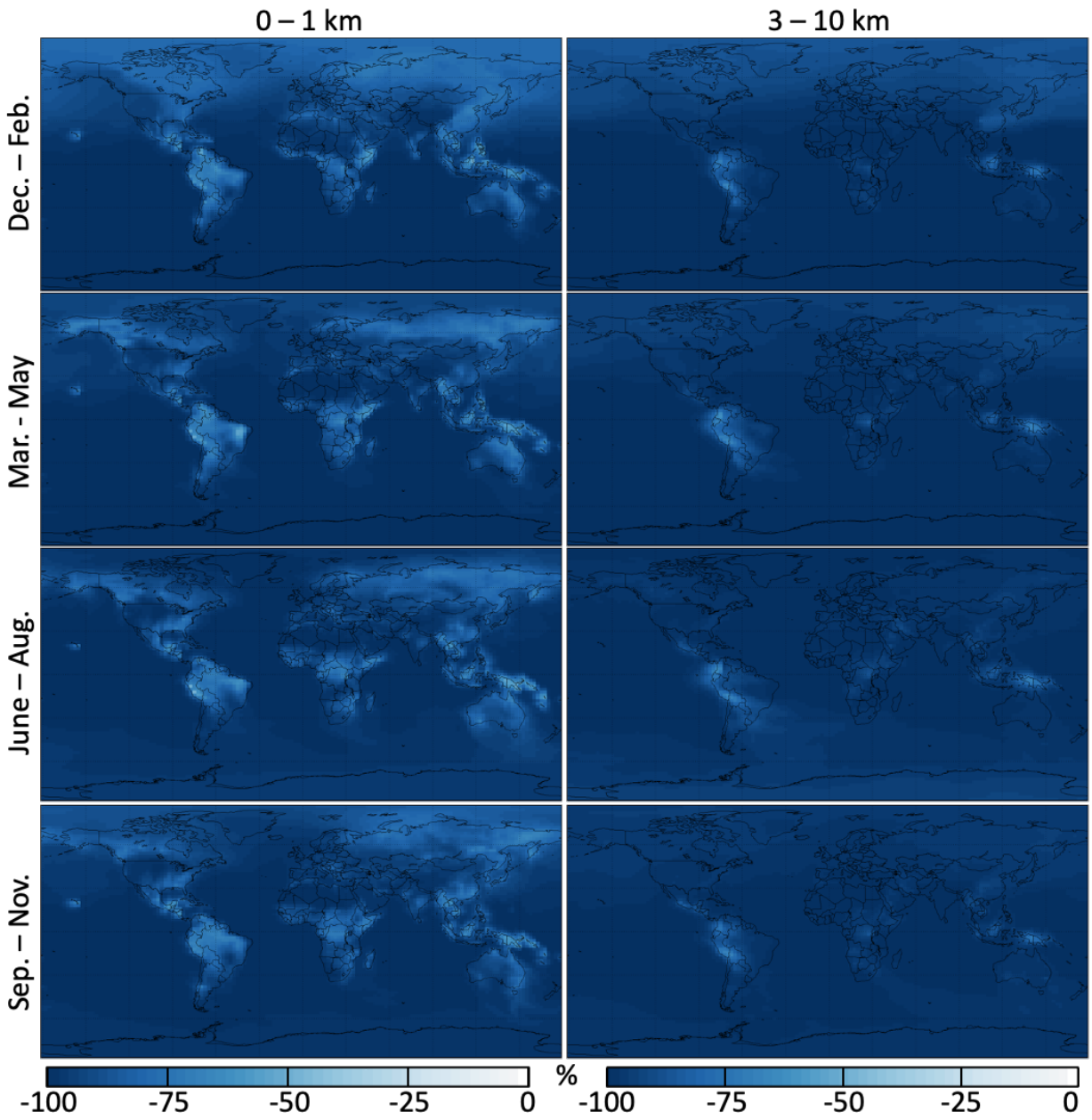

Figure S10. Percent changes in the seasonal average concentrations of first-generation IEPOX-derived organic aerosol (including only 2-MT and 2-MTS) between simulations with the base GEOS-Chem mechanism and the updated mechanism including 2-MT and 2-MTS oxidation.

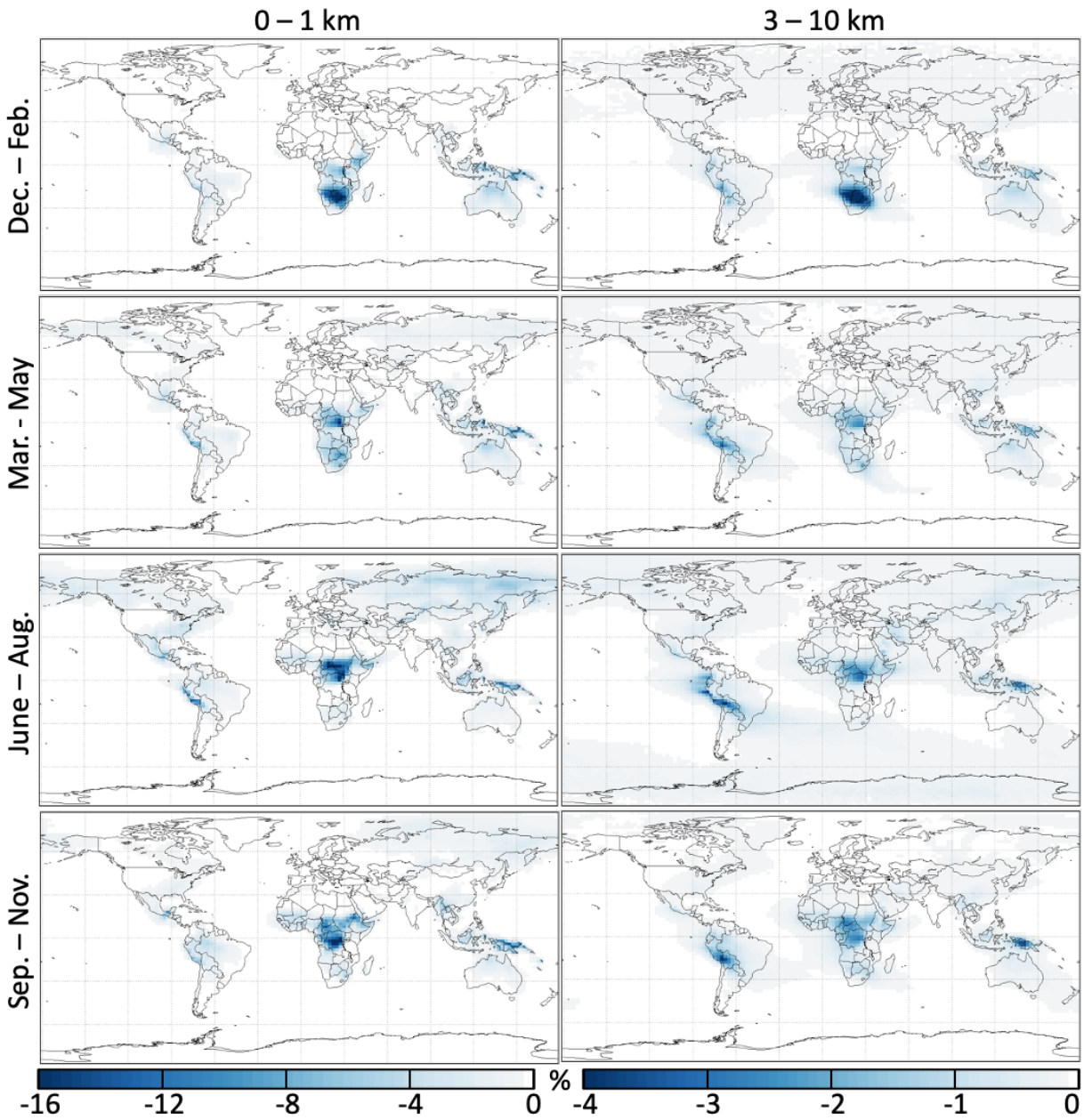

Figure S11. Percent changes in seasonally averaged OH mixing ratios at altitudes of 0 – 1 km (left) and 3 – 10 km (right) between the base GEOS-Chem mechanism and the updated mechanism with 2-MT and 2-MTS oxidation.

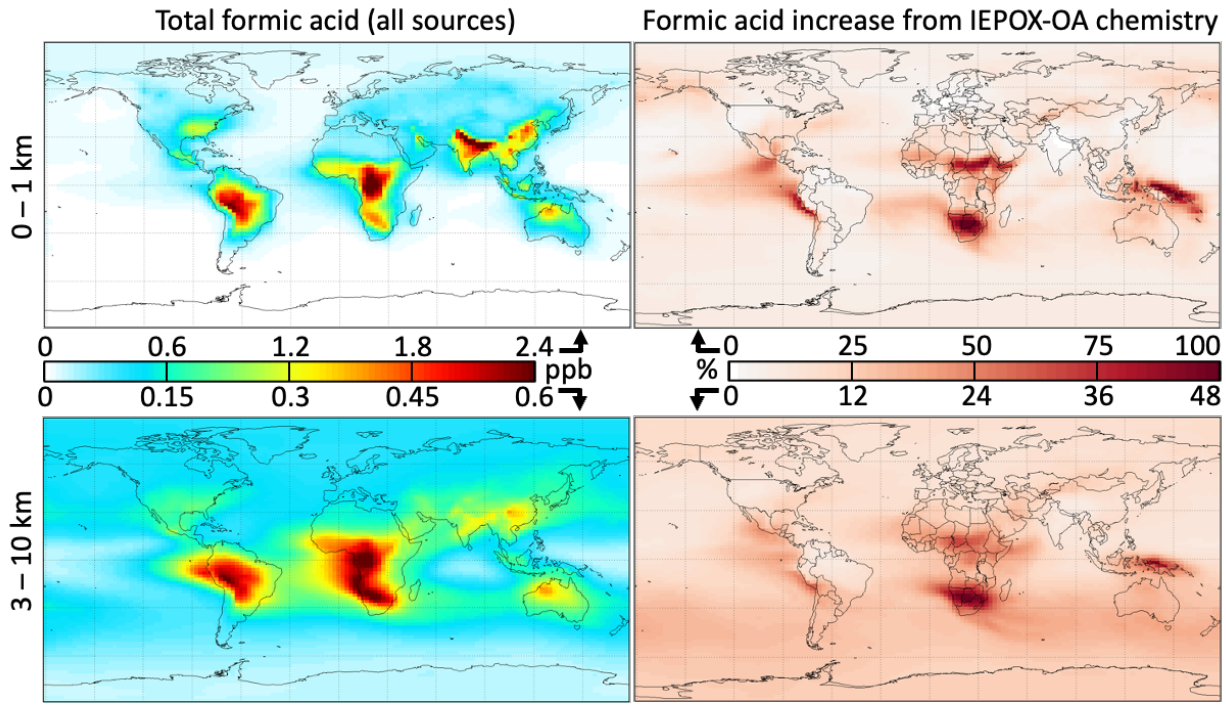

Figure S12. Total formic acid mixing ratios from all sources in a GEOS-Chem simulation with the updated 2-MT and 2-MTS oxidation mechanism (left) and the percent increase in formic acid mixing ratios when 2-MT and 2-MTS oxidation is included in GEOS-Chem (right). All maps show annual averages at altitudes of 0 – 1 km (top) or 3 – 10 km (bottom).

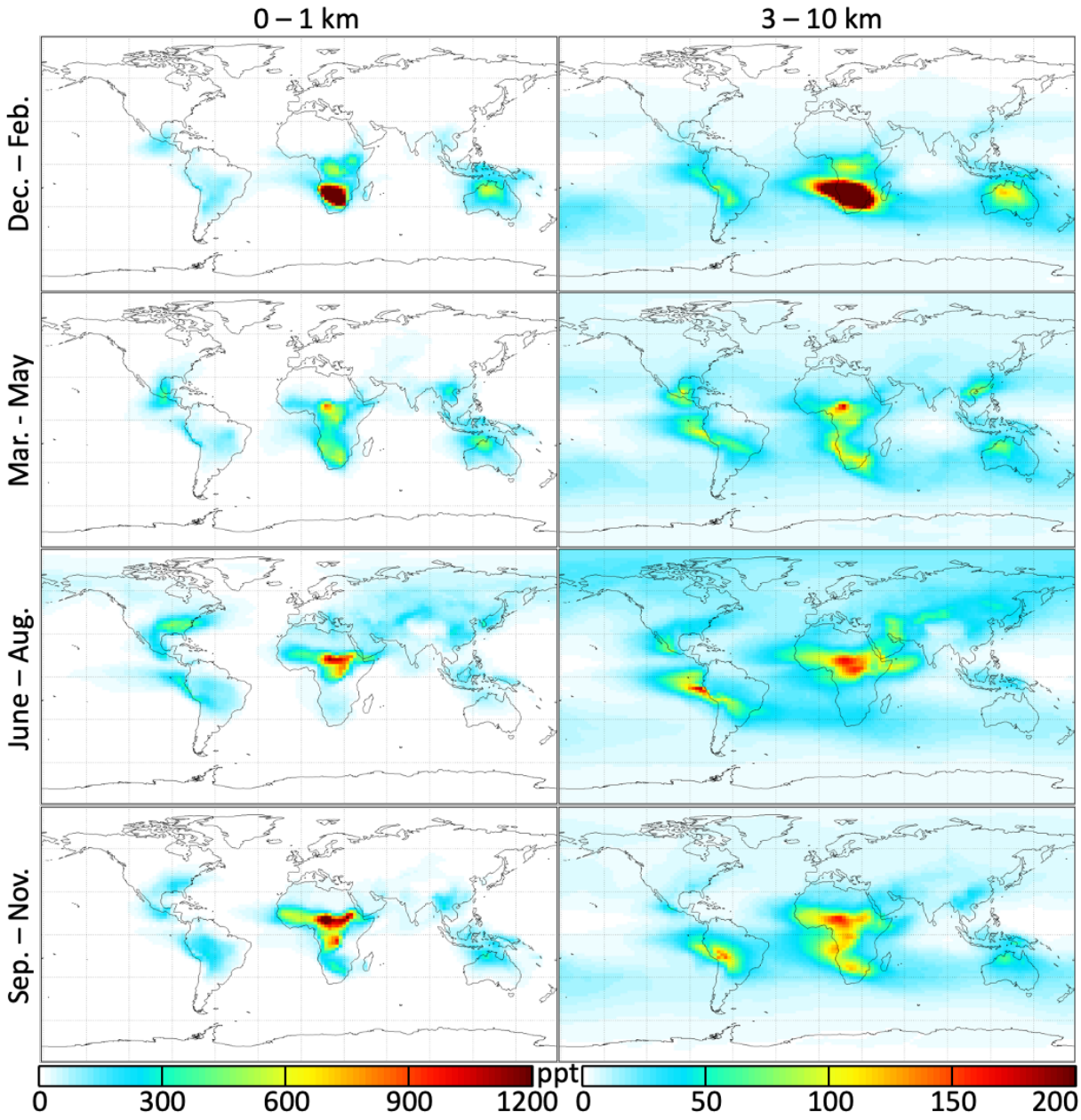

Figure S13. Seasonally averaged mixing ratios of formic acid produced from the multigenerational oxidation of IEPOX-derived organic aerosol at altitudes of 0 – 1 km (left) and 3 – 10 km (right).

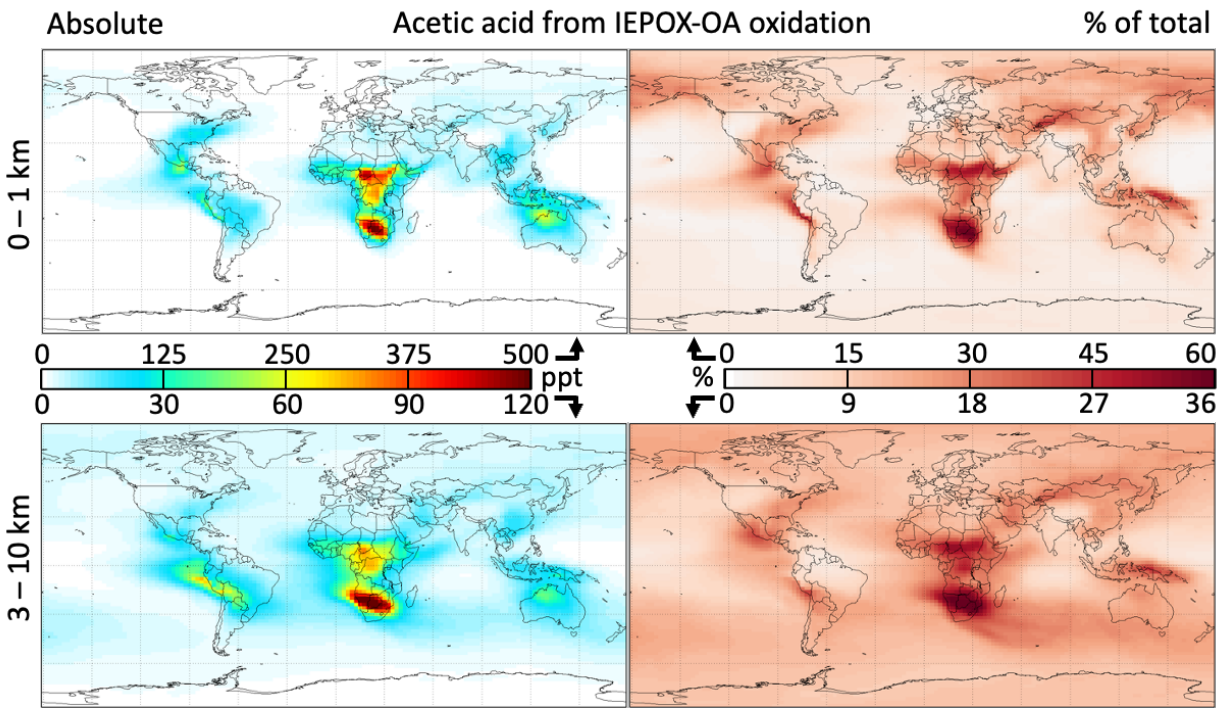

Figure S14. Like Figure 5 in the main text, but for acetic acid instead of formic acid: Acetic acid from the multigenerational oxidation of 2-MT and 2-MTS. Panels show the absolute mixing ratios of acetic acid produced from IEPOX-derived organic aerosol (IEPOX-OA) oxidation (left) and the fraction of the total acetic acid mixing ratios that this IEPOX-OA-derived acetic acid comprises (right) at altitudes of 0 – 1 km (top) and 3 – 10 km (bottom). All maps show annual averages from a GEOS-Chem simulation with the updated 2-MT and 2-MTS oxidation mechanism.

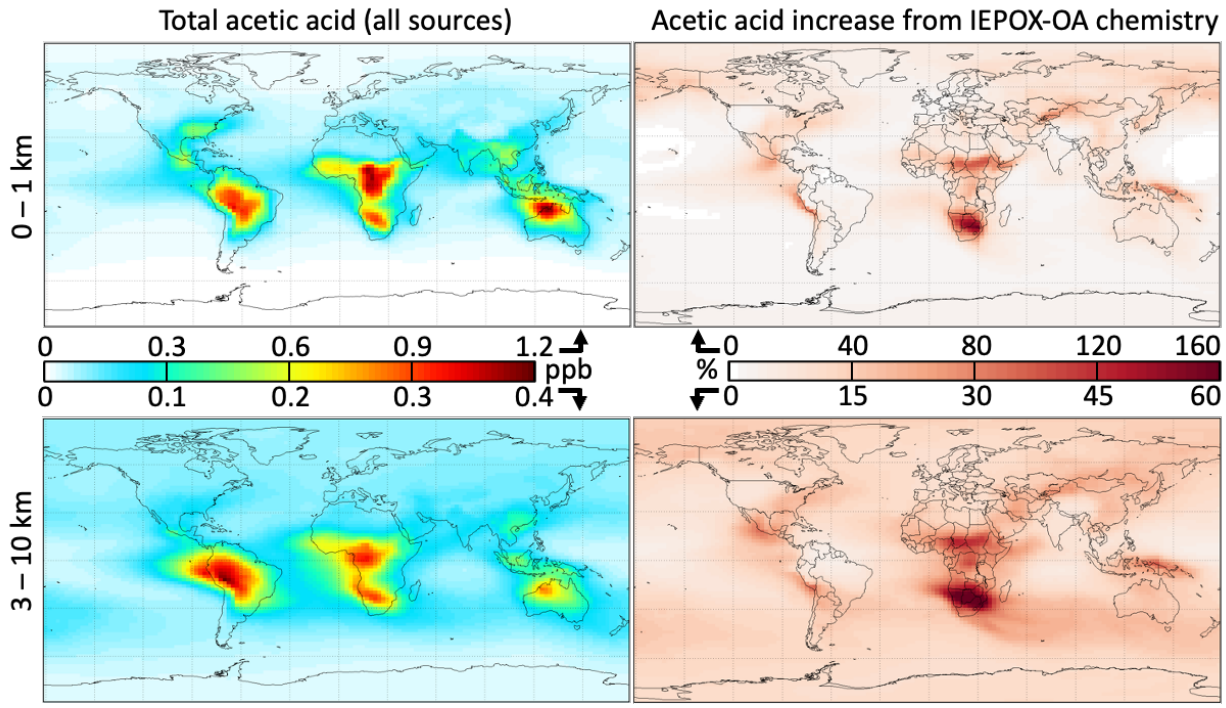

Figure S15. Like Figure S11, but for acetic acid instead of formic acid: Total acetic acid mixing ratios from all sources in a GEOS-Chem simulation with the updated 2-MT and 2-MTS oxidation mechanism (left) and the percent increase in acetic acid mixing ratios when 2-MT and 2-MTS oxidation is included in GEOS-Chem (right). All maps show annual averages at altitudes of 0 – 1 km (top) or 3 – 10 km (bottom).

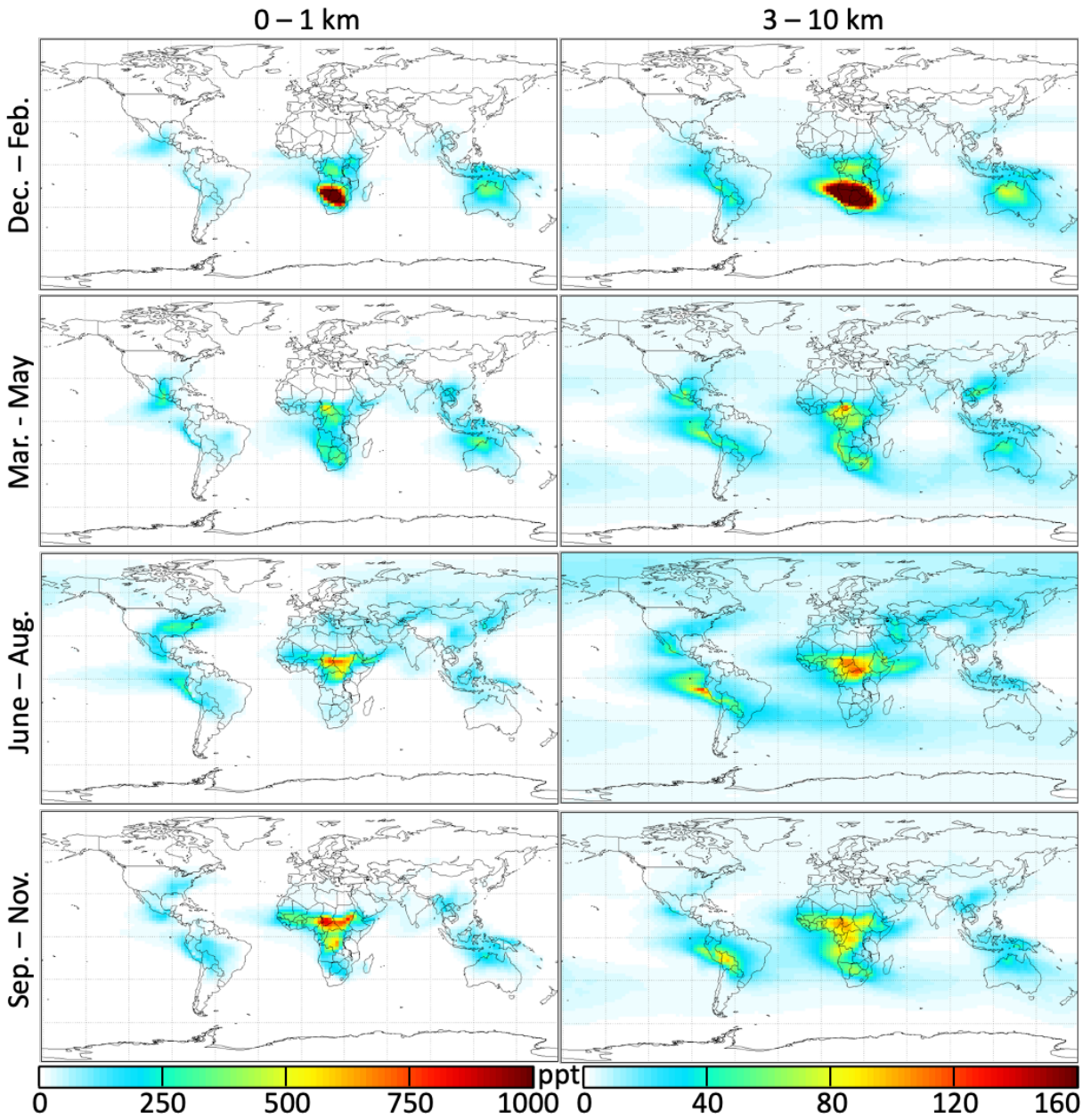

Figure S16. Like Figure S12, but for acetic acid instead of formic acid: Seasonally averaged mixing ratios of acetic acid produced from the multigenerational oxidation of IEPOX-derived organic aerosol at altitudes of 0 – 1 km (left) and 3 – 10 km (right).

Table S1. Global annual tropospheric production, emission, and fractional burden of formic acid from various sources in the GEOS-Chem simulation with the added 2-MT and 2-MTS oxidation mechanism.

Source	**Production or emission (Tg a^{-1})**	**Contribution to tropospheric burden (%)**
Primary (emissions)		
Fires	1.5	1.4
Anthropogenic	9.1	7.3
Biogenic	3.5	2.3
Secondary (production)		
2-MT & 2-MTS chemistry	14.2	12.9
Terminal alkene ozonolysis[a]	21.0	18.1
Other secondary production[b]	44.3	58.0
Total	93.6	100

[a]Including direct production from the C_1 Criegee Intermediate and indirect production via hydroxymethyl hydroperoxide (HMHP); [b]Including 29.3 Tg a^{-1} from glycolaldehyde + OH, 4.9 Tg a^{-1} from hydroxyacetone + OH, 3.1 Tg a^{-1} from acetaldehyde photolysis, 2.9 Tg a^{-1} from acetylene + OH, 2.7 Tg a^{-1} from C_4-C_5 intermediates in aromatic oxidation, and 1.4 Tg a^{-1} from C_4-C_5 intermediates in isoprene oxidation.

Mechanism S1. Reactions used to simulate NMR experiments of 2-MTS in the kinetic model and added to GEOS-Chem for global simulations. Species used include formic acid (FA), acetic acid (AA), non-specific first- (Int1) and second-generation (Int2) aqueous intermediates, and a non-specific unreactive final product to represent the leftover carbon that does not form FA and AA (FP1), which is only included in GEOS-Chem, not the kinetic modeling. The aqueous reactions of FA and AA with OH are only included in the kinetic model, not GEOS-Chem. The rate of the 2-MTS + OH reaction is from Abellar et al.;[1] those of FA and AA + OH are from Chin & Wine;[2] those of Int1 and Int2 + OH are adjusted to fit experimental data. The mechanism also uses known HO_x reactions (OH + H_2O_2, HO_2 + HO_2, OH + HO_2, H_2O_2 photolysis) and measured light flux (**Fig. S1**, scaled linearly to match oxidation rate) to initiate radical production.

2-MTS + OH → 0.2 FA + Int1	$k = 1.52\times10^{9}$ M^{-1} s^{-1}
Int1 + OH → 0.4 AA + Int2	$k = 7.6\times10^{8}$ M^{-1} s^{-1}
Int2 + OH → 1.8 FA + 0.6 AA + FP1	$k = 7.6\times10^{8}$ M^{-1} s^{-1}
FA + OH → CO_2	$k = 1\times10^{8}$ M^{-1} s^{-1}
AA + OH → CO_2	$k = 1.7\times10^{7}$ M^{-1} s^{-1}

Reactions from Cope et al.[3] used to model 2-MT reactivity are also added to GEOS-Chem in this work (Int3 and Int4 represent additional non-specific aqueous intermediates):

2-MT + OH → 0.1 FA + 0.05 AA + Int3	$k = 1.14\times10^{9}$ M^{-1} s^{-1}
Int3 + OH → 0.4 FA + 0.25 AA + Int4	$k = 3.6\times10^{8}$ M^{-1} s^{-1}
Int4 + OH → FA + AA + 0.9CO_2	$k = 1.6\times10^{8}$ M^{-1} s^{-1}

In GEOS-Chem, the non-specific intermediates and products are assigned molecular formulas to represent the carbon remaining from their precursors that has not yet fragmented to form FA or AA, which are then used to compute the organic aerosol mass. These intermediates and products are assumed to be more oxidized than their precursors and are assigned O:C and H:C ratios accordingly. These formulas are not meant to represent actual species, but rather the approximate elemental ratios of aqueous products remaining at each reaction step.

Species	Formula equivalent	MW
2-MTS	$C_5H_{11}O_7S$	215.15
Int1	$C_{4.8}H_{10.2}O_8S$	227.94
Int2	$C_4H_7O_8S$	215.12
FP1	CHO_5S	125.07
2-MT	$C_5H_{12}O_4$	136.09
Int3	$C_{4.8}H_{11.2}O_5$	148.89
Int4	$C_{3.9}H_{7.8}O_{4.8}$	131.46

Additional reactions of 1,2-dihydroxy isoprene (IDIOL) from Bates et al.[4] listed below are also added to GEOS-Chem in this work (abbreviations from GEOS-Chem are listed below reactions; T represents temperature in Kelvin):

$IDIOL + OH = IDIOLO_2$	$k = 1.14\times10^{-11}\times e^{(390/T)}$ cm^3 molecule^{-1} s^{-1}
$IDIOL + O_3 = 0.6\ CH_2OO + 0.4\ CH_2O +$ $0.6\ MVKDH + 0.4\ MCO_3 +$ $0.4\ GLYC + 0.28\ OH + 0.16\ HO_2$	$k = 5.5\times10^{-15}\times e^{(-1880/T)}$ cm^3 molecule^{-1} s^{-1}
$IDIOLO_2 + HO_2 = OH + HO_2 + 0.5\ MVKDH +$ $0.5\ CH_2O + 0.5\ GLYC + 0.5\ HAC$	$k = 2.12\times10^{-13}\times e^{(1300/T)}$ cm^3 molecule^{-1} s^{-1}
$IDIOLO_2 + NO = OH + NO_2 + 0.5\ MVKDH +$ $0.5\ CH_2O + 0.5\ GLYC + 0.5\ HAC$	$k = 2.67\times10^{-12}\times e^{(365/T)}$ cm^3 molecule^{-1} s^{-1}

Abbreviations:
IDIOL = 1,2-dihydroxy isoprene
$IDIOLO_2$ = peroxy radical from IDIOL
CH_2OO = C_1 Criegee intermediate
CH_2O = formaldehyde
GLYC = glycolaldehyde
HAC = hydroxyacetone
MCO_3 = acetylperoxy radical
MVKDH = 1,2-dihydroxybutan-3-one

REFERENCES

1. Abellar, K. A., Cope, J. D., and Nguyen, T. B.: Second-order kinetic rate coefficients for the aqueous-phase hydroxyl radical (OH) oxidation of isoprene-derived secondary organic aerosol compounds at 298 K. *Environ. Sci. Technol.*, 55 (20), 13728-13736. DOU: 10.1021/acs.est.1c4606, 2021.
2. Chin, M.; Wine, P. H. A Temperature-Dependent Competitive Kinetics Study of the Aqueous-Phase Reactions of OH Radicals with Formate, Formic Acid, Acetate, Acetic Acid, and Hydrated Formaldehyde. In *Aquatic and Surface Photochemistry*; Heiz, G. R., Zepp, R. G., Crosby, D. G., Eds.; CRC Press: Boca Raton, FL; Chapter 5, p 85, DOI: 10.1201/9781351069847-6, 1994.
3. Cope, J. D., Abellar, K. A., Bates, K. H., Fu, X., and Nguyen, T. B.: Aqueous photochemistry of 2-methyltetrol and erythritol as sources of formic acid and acetic acid in the atmosphere. *ACS Earth Space Chem.,* 5 (6), 1265-1277, DOI: 10.1021/acsearthspacechem.1c00107, 2021.
4. Bates, K. H., Cope, J. D., and Nguyen, T. B.: Gas-phase oxidation rates and products 1,2-dihydroxy isoprene. *Environ. Sci. Technol.*, 55, 14294-14304. DOI: 10.1021/acs.est.1c04177, 2021.